Available online at www.sciencedirect.com

ScienceDirect

Journal homepage: www.elsevier.com/locate/cortex

The cortical face network of the prosopagnosic patient PS with fast periodic stimulation in fMRI

Xiaoqing Gao [a,b], *Quoc C. Vuong* [c] *and Bruno Rossion* [b,d,e,*]

[a] *Center for Psychological Sciences, Zhejiang University, China*
[b] *Psychological Sciences Research Institute, Institute of Neuroscience, University of Louvain, Belgium*
[c] *Institute of Neuroscience, Newcastle University, UK*
[d] *Université de Lorraine, CNRS, CRAN, Nancy, France*
[e] *Université de Lorraine, CHRU-Nancy, Service de Neurologie, Nancy, France*

ARTICLE INFO

Article history:
Received 15 March 2018
Reviewed 4 July 2018
Revised 1 September 2018
Accepted 7 November 2018
Action editor Jason Barton
Published online xxx

Keywords:
Prosopagnosia
fMRI
Face categorization
Individual face discrimination

ABSTRACT

Following brain damage, the patient PS suffers from selective impairment in recognizing individuals by their faces, i.e., prosopagnosia. Her case has been documented in more than 30 publications to date, informing about the nature of individual face recognition and its neural basis. Here we report new functional neuroimaging data obtained on PS with a recently developed fast periodic stimulation functional imaging (FPS-fMRI) paradigm combining high sensitivity, specificity and reliability in identifying the cortical face-selective network (Gao et al., 2018). We define the extent of the large and reliable face-selective activation in the lateral section of the right middle fusiform gyrus, i.e., right FFA, which forms a single cluster of activation lying at the anterior border of the patient's main lesion in the inferior occipital gyrus. The contribution of posterior face-selective responses in the right or left inferior occipital gyrus is ruled out, strongly supporting the view that face-selective activity emerges in the right middle fusiform gyrus of the patient's brain from non-face-selective inputs from early visual areas. Despite this, low-level visual cues, i.e., amplitude spectrum of images, do not contribute to neural face-selective responses anywhere in the patient's cortical face network. This sensitive face-localizer approach also reveals an intact face-selective network anterior to the fusiform gyrus, including clusters in the ventral anterior temporal lobe (occipito-temporal sulcus and temporal pole) and the inferior frontal gyrus, with a right hemispheric dominance. Overall, with the exception of the left inferior occipital gyrus, the cortical face network of the prosopagnosic patient PS appears remarkably similar to typical individuals in non-brain damaged regions. However, unlike in neurotypical adults tested in the present study, including age-matched controls, a novel paradigm based on FPS-fMRI confirms that the patient's face network is insensitive to differences between rapidly presented pictures of unfamiliar individual faces, in line with her prosopagnosia.

* *Corresponding author*. CRAN, Université de Lorraine, CNRS, 2 Avenue de la Forêt de Haye, BP 90161, 54500, Vandoeuvre-Les-Nancy, France.
E-mail address: Bruno.rossion@uclouvain.be (B. Rossion).

https://doi.org/10.1016/j.cortex.2018.11.008
0010-9452/

1. Introduction

"Prosopagnosia" (from the Greek "prosopon", *face*, and "a-gnosia", *without knowledge*) is a term used in both the scientific and public community referring to the subjective or objective difficulties at recognizing individuals by their face, with or without neurological cause. This condition was originally defined in the context of agnosia: a neurological deficit of recognition limited to one modality (i.e., vision), which cannot be accounted for by sensory (visual) defects and/or intellectual impairments. In prosopagnosia, the visual recognition deficit is thought to be limited (i.e., selective) to one category: faces (Bodamer, 1947). So-defined classical cases of prosopagnosia are in fact extremely rare, and given the specificity of their impairment, they can be highly informative to understand not only the nature of human individual face recognition but also its neural basis (e.g., Barton, 2008; Rossion, 2014; Sergent & Signoret, 1992; Young, 2011). Here we report an updated investigation of the cortical face network of a classical case of prosopagnosia reported in many studies (since Rossion et al., 2003). PS sustained a severe closed head injury in 1992, just before her 42nd birthday. Since her accident and to this date, her only continuing complaint concerns her profound difficulty at recognizing individuals by their face, including those of family members, as well as her own. Specifically, PS neither complains nor presents any difficulty at recognizing non-face objects in her daily activities and in laboratory experiments. Her case has been described extensively in previous publications spanning from 2003 to 2018, i.e., about 30 publications in total, reflecting over 18 years of testing (see Rossion, 2014 for review; and Ramon, Busigny, Gosselin, & Rossion, 2016 for more recent references). To our knowledge, PS is by far the most documented case of prosopagnosia in the scientific literature.

Although PS's brain lesions are bilateral and cannot be taken as supporting the well-known right hemispheric dominance in prosopagnosia and individual face recognition (Hecaen & Angelergues, 1962; Meadows, 1974; Bouvier & Engel, 2006), her pattern of brain damage has been particularly informative because the ventral occipito-temporal lesions are asymmetrical, sparing the cortical territory of the right lateral middle fusiform gyrus (Fig. 1). This region typically includes the so-called "Fusiform Face Area" ("FFA", Kanwisher, McDermott, & Chun, 1997), a region that is activated more by faces than by non-face visual objects during functional magnetic resonance imaging (fMRI) (see Sergent, Shinsuke, & Macdonald, 1992 for initial evidence using positron emission tomography, PET; see Puce, Allison, Gore, & McCarthy, 1995 in fMRI). This functional brain region has been investigated for two decades in neuroimaging (Kanwisher, 2017), recently highlighted as the most selective region with direct neural intracerebral recordings (Jonas et al., 2016) and proved to be critically involved in (individual) face perception (Parvizi et al., 2012; Rangaranjan & Parvizi, 2014; Jonas et al., 2018). Yet, despite the patient's prosopagnosia, and a large posterior lesion in the right inferior occipital gyrus, PS's brain includes an FFA in the right hemisphere with the extent and height of activation not differing from normal controls (Rossion et al., 2003), a finding repeatedly confirmed in neuroimaging investigations of the patient's brain (Dricot, Sorger, Schiltz, Goebel, & Rossion, 2008; Righart, Andersson, Schwartz, Mayer, & Vuilleumier, 2010; Rossion, Dricot, Goebel, & Busigny, 2011; Schiltz et al., 2006; Sorger, Goebel, Schiltz, & Rossion, 2007).

Together with further observations on PS as well as replications in other brain-damaged patients (Steeves et al., 2006; Weiner et al., 2016), this finding has constrained and inspired human neurofunctional models of face processing. Indeed, in the original neurofunctional model of Haxby and colleagues (2000; see also Ishai, 2008; Fairhall & Ishai, 2007), face-selectivity in the middle fusiform gyrus was thought to originate from feedforward face-selective inputs originating from the inferior occipital gyrus (IOG, "Occipital Face Area", OFA). However, thanks to neuroimaging findings made in PS

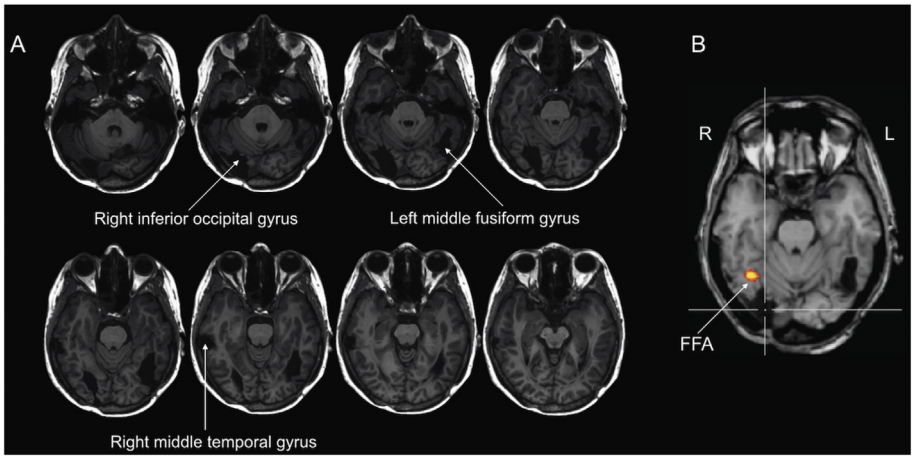

Fig. 1 – The extent of cortical lesion and functional activation to faces in the brain of patient PS. PS acquired severe brain damage mainly in the right inferior occipital gyrus and the left middle fusiform gyrus. The full extent of the lesion is shown as black hollows in the group of axial slices with a gap of 3 mm between neighboring slices (A). Despite extensive brain damage, face-selective responses (B) – here the yellow spot of activation above threshold from the original report (Rossion et al., 2003) – are observed in the right middle fusiform gyrus ("Fusiform face Area", FFA).

Please cite this article as: Gao, X et al., The cortical face network of the prosopagnosic patient PS with fast periodic stimulation in fMRI, Cortex, https://doi.org/10.1016/j.cortex.2018.11.008

in particular, as well as other pieces of evidence (Gentile & Rossion, 2017; Jiang et al., 2011), it is now generally acknowledged that face-selectivity in the middle fusiform gyrus can emerge from inputs from early (non-face-selective) visual areas (Duchaine & Yovel, 2015; Rossion, 2008).

Here we take advantage of the recent development of a highly sensitive, specific, and reliable approach based on fast periodic stimulation in fMRI (FPS-fMRI, Gao, Gentile, & Rossion, 2018) to provide an updated view on PS's cortical face network, strengthening previous findings and clarifying a number of issues. Specifically, the study pursued 6 objectives. First, we test whether typical face-selective responses can be observed in the patient's brain for faces presented extremely rapidly, i.e., allowing only one fixation per face. We recently provided evidence for such responses on the patient's scalp using the fast periodic visual stimulation (FPVS) in EEG (Liu-Shuang, Torfs, & Rossion, 2016). However, the scalp topography of the response was different in PS than in the control individuals tested (i.e., with a stronger left occipito-temporal lateralization, see Figure 9 in Liu-Shuang et al., 2016), an observation that was also made earlier for face-selective EEG responses with a more conventional approach (Alonso-Prieto et al., 2011). This difference in spatial topography has been attributed to a distortion of the outward flux of currents due to brain damage rather than differences in the localization of the remaining underlying cortical sources (Liu-Shuang et al., 2016). Testing the same paradigm with the sensitive FPS-fMRI will elucidate whether the localization of non-damaged face-selective regions is not different in the patient than in typical individuals.

Second, we provide a stringent test for the contribution of low-level visual information to face-selective responses by comparing a FPS stimulation with natural images of faces to the same stimulation with phase-scrambled images, preserving amplitude spectrum (Gao et al., 2018; Rossion, Torfs, Jacques, & Liu-Shuang, 2015). This test will evaluate whether face-selective activation in PS's brain can be attributed even partly to low-level visual information in the stimuli. Such control has become important in light of relatively recent claims that category-selective responses in high-level regions obtained in fMRI with classical face and object localizers could be partly, or mainly, due to low-level visual cues preserved by phase-scrambling of the stimuli (i.e., amplitude spectrum; Andrews, Watson, Rice, & Hartley, 2015; Watson, Young, & Andrews, 2016).

Third, we take advantage of the high sensitivity (i.e., SNR) of the novel FPS-fMRI approach and the objectivity of identification of the response of interest (i.e., at a predetermined frequency) to quantify and define the spatial *extent* of the right lateral fusiform gyrus selective response to faces with respect to the patient's posterior lesion in the right inferior occipital gyrus. Because applying a single statistical threshold cannot reflect the continuous nature of the degree of face-selective activation, we plotted the activation with several levels of threshold to provide a better view of the spatial extent of activation in the right lateral fusiform gyrus.

Fourth, we further test for the presence or absence of ventral face-selective responses posterior to the right FFA, either in the right or left hemisphere of the patient's brain. In one previous study using a traditional face localizer, which was less sensitive and specific, there was a small face-selective region in the left inferior occipital gyrus, which was tentatively termed as a left OFA (Sorger et al., 2007). However, this cluster was localized more posteriorly than in typical individual brains, and not observed in any other neuroimaging studies of the patient. This is an important issue to rule out potential contributions of face-selective inputs from the left inferior occipital gyrus to the contralateral (i.e., right) cortical face network. Here, we aim to resolve this issue with a more effective fMRI paradigm than used in previous studies.

Fifth, we test for the presence or face-selective responses in the ventral anterior temporal lobe of PS's brain, including the temporal pole. Since previous reports of the patient in neuroimaging, there has been an increased focus on face-selective regions located anteriorly to the FFA, in the ventral anterior temporal lobe (Rajimehr, Young, & Tootell, 2009; Nasr & Tootell, 2012; Von Der Heide, Skipper, & Olson, 2013; Collins & Olson, 2014; Jonas et al., 2015; Collins, Koski, & Olson, 2016; Yang, Susilo, & Duchaine, 2016). This issue is also important to address here, especially since a review of face processing claimed that PS had damage in the right anterior temporal lobe, potentially contributing to her prosopagnosia (Pitcher et al., 2011). Contrary to this claim, anatomically, the whole ventral visual stream anterior to the right inferior occipital gyrus appears intact in the patient's brain (Fig. 1), and one should therefore expect face-selective regions anterior to the FFA in the patient's ventral anterior temporal lobe. Since the FPS-fMRI paradigm reveals ventral anterior temporal lobe face-selective responses in many individual brains (Gao et al., 2018) despite the signal drop-out in this region due to magnetic susceptibility artifacts (Rajimehr et al., 2009; Wandell, 2011; Axelrod & Yovel, 2013; Jonas et al., 2015; see discussion in; Rossion, Jacques, & Jonas, 2018), the presence or absence of face-selective activation in this region will help understanding whether functional abnormality in the ventral anterior temporal lobe potentially contributes to PS's prosopagnosia.

Finally, in previous reports using fMRI-adaptation designs, there was no evidence of release from adaptation to identity in the patient's FFA or other identified face-selective regions (Dricot et al., 2008; Schiltz et al., 2006; Steeves et al., 2009), in line with her prosopagnosia. Here we also developed and tested a complementary FPS approach in fMRI, based on previous EEG studies (Liu-Shuang et al., 2014, 2016) to assess PS's lack of sensitivity to differences in individual faces in her whole cortical face network. This test should provide direct evidence regarding the neural response (or lack of) to individual faces in the patient's brain. Conversely, given the patient's severe and selective deficit in individual face recognition, the study can serve as a validation of this new paradigm in fMRI.

The highly selective impairment in individual face recognition alone with focal brain damage in the rare and unique case of PS provides us an invaluable opportunity to study the organization of the cortical face-processing network, in particular the interdependency of the brain regions involved in face processing. It also provides us with an opportunity to validate a novel measure of individual face discrimination in fMRI, testing the hypothesis that the response in the patient's brain should be smaller or even absent as compared to normal observers.

Please cite this article as: Gao, X et al., The cortical face network of the prosopagnosic patient PS with fast periodic stimulation in fMRI, Cortex, https://doi.org/10.1016/j.cortex.2018.11.008

2. Material and methods

2.1. Patient PS

Patient PS is a right-handed female born in 1950 who suffered a closed-head injury in 1992. She was tested in the present study in 2016 at the age of 65 years. Since her accident and to this date, her only continuing complaint concerns her profound difficulty at recognizing individuals by their face, including those of family members, as well as her own. To determine a person's identity, she usually relies on contextual information, her excellent memory, and non-facial cues such as the person's voice, posture, or gait, etc. However, she may also use sub-optimal facial cues such as the mouth (Caldara et al., 2005; Ramon et al., 2016). Providing that there is no context given, i.e., that she does not expect to be shown only the pictures of specific people that she is supposed to know, and that the stimuli are carefully controlled, her recognition of pictures of familiar faces is close to zero (Busigny et al., 2014; Ramon et al., 2016; Rossion et al., 2003). When PS knows a well-defined set of familiar people's faces that are shown to her as pictures, she can perform better and recognize some of the faces. However, she then takes an extremely long time relative to controls to scrutinize each face and make guesses about who the person is (see Ramon et al., 2016). She is also close to chance level at distinguishing personally familiar from unfamiliar faces (Busigny & Rossion, 2010; Ramon et al., 2016), and she is also severely impaired at individual face matching tasks such as in the Benton Face Recognition Test (BFRT, Benton & Van Allen, 1972; see Busigny & Rossion, 2010), or impaired at explicit encoding and recognition of individual faces among distractors as in the Cambridge Face Memory Test (CFMT, Duchaine & Nakayama, 2006; see Ramon et al., 2016; see Appendix for descriptions of the BFRT and the CFMT tests).

Her performance at standard clinical and neuropsychological tests of visual perception/recognition was initially reported in Table 1 of Rossion et al. (2003) and Sorger et al. (2007). PS's color vision is in the low normal range (Sorger et al., 2007). Her visual field is almost full (with exception of a small left paracentral scotoma; of about 2–3° by 3°, see also Sorger et al., 2007), and her visual acuity is in the lower range.

Despite this scotoma, PS neither complains nor presents any difficulty at recognizing nonface objects in real life and in the laboratory (Rossion, 2018; Rossion et al., 2003). PS performs accurately and quickly at naming fruits and vegetables, which often have similar shapes, and whose recognition is often impaired in other cases of reported prosopagnosia (e.g., 9 out of 10 patients reported in Barton et al., 2008). In computer experiments, PS was able to discriminate exemplars of nonface categories as accurately and rapidly as age-matched controls (e.g., cars, birds, boats, houses; Schiltz et al., 2006; see also Rossion, 2018) and did not show any abnormal increase in error rates and RTs with increasing levels of physical similarity between object targets and distractors in matching tasks (Busigny, Graf, Mayer, & Rossion, 2010).

2.2. Typical adult participants and elderly participants

We performed data collection at the Maastricht Brain Imaging center (Maastricht, the Netherlands) and recruited control participants from the local community. We included a pool of nine typical adults (mean age = 27.1 ± 4.9 years, range = 21–34 years, 6 females) to compare to PS's response in the paradigm testing for neural individual face discrimination. In addition to the typical (young) adults, we also included 4 healthy elderly adults (mean age 64.0 ± 2.0 years, range = 61–65 years, 3 females) to test the possibility that age-related decline in individual face recognition (e.g., Germine, Duchaine, & Nakayama, 2011) may contribute to any differences found between the young adults control group and PS. None of the participants reported any history of brain damage or psychiatric or neurological disorders, or current use of any psychoactive medications. All the typical participants had normal or corrected-to-normal vision and were right-handed. The research protocols were in accordance with the ethical standards of the research ethics committees of the University of Louvain and with the 1964 Helsinki declaration and its later amendments or comparable ethical standards. No part of the study procedures or analysis was pre-registered prior to the research being conducted. We obtained informed written consent from all the participants prior to the experimental sessions. Younger participants received monetary compensation for their participation in the study.

2.3. Scanning procedures

2.3.1. Stimuli

Fig. 2 illustrates the fast periodic stimulation paradigm with examples of the stimuli used in the present study, which consisted of color images of faces and non-face objects from a variety of categories (e.g., houses, animals, cars). There were two different sets. The first stimulus set included natural images of 100 faces and 200 non-face objects with a wide range of variation in size, lighting conditions, and position of the face and object within the image from Gao et al. (2018; Fig. 2B; the stimuli set along with the data and analysis code from the current study are available upon request). Each face image contained only a single face. Each non-face object image contains one main object in the foreground. The second stimulus set consisted of color images of 25 Caucasian male faces with a neutral expression placed against a grey background as used in Liu-Shuang et al. (2014; Fig. 2C). The faces were presented from the frontal view with external features, such as ears and hair, removed using Adobe Photoshop. The faces were taken under standardized conditions with the same lighting, background, and distance from the camera.

All images were back-projected onto a projection screen by an MRI compatible LCD projector placed 75 cm from the screen. Participants viewed the images through a mirror placed within the RF head coil. The screen subtended a viewing angle of 14.6° × 14.6° (19.2 × 19.2 cm). The experiment and response collection was controlled by a stimulation program running in Java.

Please cite this article as: Gao, X et al., The cortical face network of the prosopagnosic patient PS with fast periodic stimulation in fMRI, Cortex, https://doi.org/10.1016/j.cortex.2018.11.008

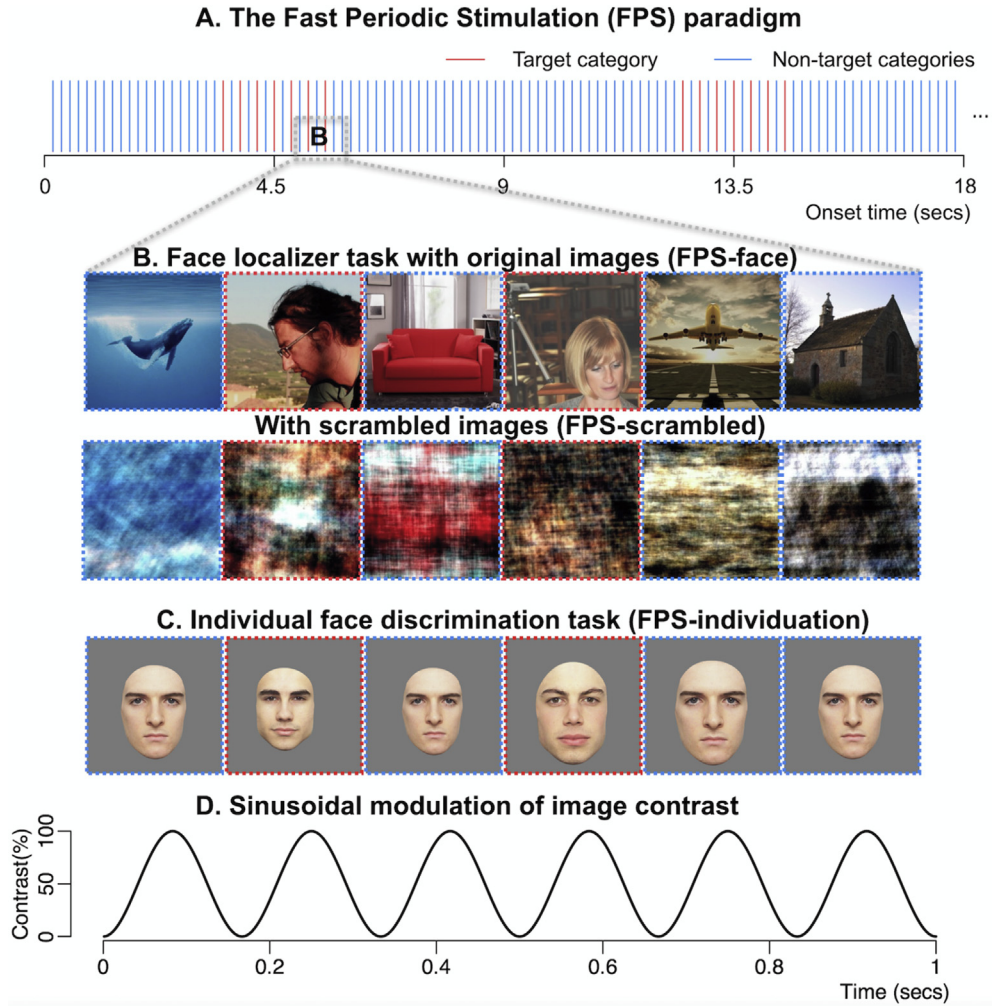

Fig. 2 – Experimental procedure. A) Images are presented at a fast rate (6 Hz). Every 9 sec, a burst of 7 images from the target category (red bins) alternates with images from the non-target categories (blue bins) for 2.167 sec. B) A 1-sec interval in the face localizer task (FPS-face), where faces are the category of interest, among non-face objects. The scrambled versions of the images are shown below their corresponding original images (FPS-scrambled). C) A 1-sec interval in the individual face discrimination task, where one individual identity (in blue frames) is presented throughout the stimulation at different sizes, and 24 other identities serve as the category of interest (in red frames) to form a direct contrast between individual faces. The sizes of the faces changed randomly up to 20% from trial to trial to minimize low-level repetition effects. D) The contrast of the images was modulated by a sinusoidal function.

2.3.2. *Experimental procedures*

We used the Fast Period Stimulation (FPS) fMRI paradigm as illustrated in Fig. 2 and described previously (Gao et al., 2018). In brief, the FPS-fMRI paradigm presents images from a category of interest (target category) and from non-target categories at a fast rate. The images from the non-target categories are presented at a base rate of 6 Hz (i.e., 6 images/sec, 2A) with a stimulus onset asynchrony (SOA) of 166.7 msec (10 screen refresh cycles at a refresh rate of 60 Hz). There is a "burst" period of the target category for 2.167 sec every 9 sec, in which a set of seven images from the target category (e.g., faces in the face localizer task) alternate with a set of seven images from the non-target categories (hence images from the target category appear at a rate of 3 Hz). These burst periods create direct contrasts between the target and non-target categories. Since the burst periods happen at a fixed frequency, the neural response related to the target category can be measured with Fourier analysis. All images are contrast modulated by a sinusoidal function to provide a smooth transition between successive images (Fig. 2D). Given the presentation parameters, participants can make only one fixation per image. Each fMRI run had a length of 396 sec so that burst periods occurred 44 times at a frequency of 1/9 Hz (i.e., .111 Hz, referred to as the stimulation frequency). For each run, images were randomly drawn from the corresponding target or non-target categories.

To localize brain regions responding more to faces than to non-face objects, we used a face-localizer stimulation sequence (FPS-face, Fig. 2B). For each run in this condition, the natural face images served as the target category whereas the non-face object images served as the non-target categories

Please cite this article as: Gao, X et al., The cortical face network of the prosopagnosic patient PS with fast periodic stimulation in fMRI, Cortex, https://doi.org/10.1016/j.cortex.2018.11.008

(Gao et al., 2018). The contribution of low-level visual cues is minimized by using highly variable images (see Rossion et al., 2015). To further control for low-level visual differences between face and object images, we presented PS with Fourier-phased scrambled versions of the natural faces and objects on separate runs using the same stimulation sequence (FPS-scrambled, Fig. 2B).

To localize brain regions selectively discriminating different faces, we used an individual face discrimination stimulation sequence (FPS-individuation, Fig. 2C), directly inspired from a paradigm validated with electroencephalography (EEG; see Liu-Shuang et al., 2014). For each run in this condition, we randomly selected one of the 25 Caucasian male faces. The remaining faces served as the target category (i.e., different facial identities throughout the run, red lines and boxes in Fig. 2) whereas the selected face served as the non-target category (i.e., same facial identity throughout the run, blue line and boxes in Fig. 2). The target faces were necessarily repeated in each run. As the target face could become familiarized as a result of repeated display, we never used the target face in one scanning run as a non-target face in a subsequent scanning run for the same participant. To minimize low-level adaptation to the small number of images, the size of the face image was randomly scaled up to 20% on a trial-by-trial basis (i.e., 90%–110% of the original image size), so that different retinal images were presented on each trial (see Liu-Shuang et al., 2014; Dzhelyova & Rossion, 2014). Two other aspects of this paradigm limit the contribution of low-level visual cues to the individual face discrimination response: First, since there are many different individual discriminations performed in a stimulation sequence, the repeated face is contrasted to *various* faces, differing in their own way in terms of low-level visual cues from the repeated face (i.e., no individual face discrimination based on specific low-level cues); Second, each image is presented only for one fixation and, given the size changes, the differences between images cannot be resolved locally. As a result, the paradigm is associated with large decreases of responses in EEG when images are presented upside-down or reversed in contrast, two manipulations that preserve low-level visual cues (see Liu-Shuang et al., 2014; Liu-Shuang et al., 2016).

As in previous studies with this approach (e.g., Gao et al., 2018; Rossion et al., 2015), we used a fixation-change task for all conditions. Importantly, the stimulus manipulation for this task was orthogonal to the main manipulation (i.e., face category or individual face change) but ensured that participants remained attentive to the visual stimulation. Participants were instructed to press a predefined key on an MRI-compatible response pad using their right index finger when they detected a color change of a central fixation cross superimposed on the images (Rossion et al., 2015). The cross subtended a visual angle of 1.2° and was highly visible to both PS and the control participants. During each run, the fixation cross changed from black to white for 200 msec (and then back to black) a total of 70 times, with the interval between any two changes randomly determined to be between 2 and 10 sec. Both PS and the control participants were very accurate in performing this task (mean accuracy = .89 ± .12 for PS and .92 ± .03 for the control participants).

2.3.3. *Order of the conditions*

PS underwent two scanning sessions separated by a short break, during which she rested outside of the scanner. In the first session, she performed two FPS-face runs alternating with two FPS-scrambled runs, followed by one anatomical scan (FPS-face, FPS-scrambled, FPS-face, FPS-scrambled, anatomical). In the second session, she performed two FPS-face runs, alternating with two FPS-individuation runs, followed by one anatomical scan (FPS-face, FPS-individuation, FPS-face, FPS-individuation, anatomical). She started both sessions with a FPS-face run. Each control participant underwent a single scanning session with two FPS-face runs alternating with two FPS-individuation runs. Across participants, the first run was randomly assigned to be either the FPS-face or FPS-individuation run. We collected an anatomical scan for each control participants after the functional runs. Each session for PS and the control participants took approximately 40 min.

2.3.4. *MR image acquisition*

We acquired the MRI images using a 3T Siemens Magnetom Prisma scanner (Siemens Medical System, Erlangen, Germany) with a 64-channel head-neck coil. Anatomic images were collected using a high-resolution T1-weighted magnetization-prepared gradient-echo image (MP-RAGE) sequence (192 sagittal slices, TR = 2,250 msec, TE = 2.21 msec, voxel size = 1 mm isotropic, FA = 9°, FoV = 256 × 256 mm^2, matrix size = 256 × 256). Functional images were collected with a T2* weighted gradient-echo echoplanar imaging (EPI) sequence (TR = 1,500 msec, TE = 30 msec, FA = 72°, voxel size = 3 mm isotropic, FoV = 240 × 240 mm^2, matrix size = 64 × 64, interleaved), which acquired 23 oblique-axial slices covering the entire occipital and temporal lobes. Each functional run took 414 secs (396 secs + 8 secs dummy scan).

2.4. *Analysis*

2.4.1. *Preprocessing*

The functional runs were motion-corrected with reference to the average image of the first functional run of the experiment using a 6-degree rigid body translation and rotation via an intra-modal volume linear registration implemented in the FMRIB Software Library (FSL, version 5.0.8, Smith et al., 2004). We next spatially smoothed the motion-corrected data with a 3-mm FWHM Gaussian kernel and removed linear trends from the preprocessed time series data of each voxel. Lastly, we converted the time series data to percentage of blood-oxygenation-level dependent (BOLD) signal change by dividing the time series of each voxel by its mean signal intensity.

2.4.2. *Magnitude of neural response*

To calculate the magnitude of neural response at the stimulation frequency (.111 Hz) in the FPS-fMRI paradigm, we followed the same procedure as described in Gao et al. (2018). First, we performed a Fast Fourier Transform (FFT) on the preprocessed BOLD time series to obtain the amplitude spectrum. Second, we calculated the mean and SD of the amplitude of the 40 frequency bins neighboring the stimulation

Please cite this article as: Gao, X et al., The cortical face network of the prosopagnosic patient PS with fast periodic stimulation in fMRI, Cortex, https://doi.org/10.1016/j.cortex.2018.11.008

frequency (20 on each side, e.g., Rossion et al., 2015; Jonas et al., 2016). Lastly, as in previous studies (McCarthy et al., 1994; Puce et al., 1995), we calculate the signal-to-noise ratio (SNR) of the response at the stimulation frequency by converting its amplitude to a z-score using the computed amplitude mean and SD from the neighboring frequencies. This procedure is applied to each voxel independently.

2.4.3. *Defining activation and deactivation of neural responses*

As in Gao et al. (2018), we defined the activation and deactivation of the neural response using the phase of BOLD response at the stimulation frequency. In general, a positive phase value indicates an increasing BOLD response amplitude after the onset of the target stimuli (e.g., faces in the FPS-face runs), whereas a negative phase value indicates a decreasing BOLD response amplitude after the onset of the target stimuli. To account for individual differences in the time to reach maximum BOLD response amplitude, for each individual we plotted the histogram (20 bins) of phase values of all the voxels with a z-score above 3 and with only a positive phase value. We used the phase value of the histogram bin that has the largest number as the center phase (φ) and defined all the voxels with their phase values within $\varphi \pm \pi/2$ as activations (+sign) and voxels with their phase values outside of this window as deactivations (− sign). We then applied the signs to the thresholded SNR (z-score) maps and obtained the final response map containing only voxels that have increased BOLD response (+sign) to the presence of the target stimuli.

2.4.4. *Averaging across scanning runs*

Across runs of the same condition, the target category was always presented at the same phase, whereas noise from other periodic sources (e.g., pulse, breathing) could have different phases across runs. Therefore, by averaging the time series across runs, we increased SNR to detect neural responses to the periodic stimulation. For PS, we averaged the data across runs and sessions as follows. To define face-selective areas, we averaged each voxel's time series across all four FPS-face runs. To compare the magnitude of neural responses between the FPS-face, FPS-individuation and FPS-scrambled conditions, we used the averaged time series across the two FPS-face runs collected in Session 1 and compared it to the averaged time series across the two runs of the FPS-scrambled (in Session 1) and FPS-individuation conditions (in Session 2). For the test-retest reliability analysis of the FPS-face condition, we compared the time series averaged across the two runs in Session 1 to the time series averaged across the two runs in Session 2. For control participants, we averaged across the two runs for both the FPS-face and FPS-individuation conditions to localize face-selective areas and compare neural responses across conditions, and we used the two FPS-face runs separately for the test-retest reliability analysis.

2.4.5. *Reliability*

We confined the test-retest reliability analysis to the anatomically defined right fusiform gyrus so that the current results are directly comparable to previously reported test-retest reliability scores (Berman et al., 2010; Duncan, Pattamadilok, Knierim, & Devlin, 2009; Kawabata Duncan & Devlin, 2011). Specifically, for each participant we first identified face-selective voxels in the right fusiform gyrus in one session using an uncorrected threshold level of $p < .0001$; then selected the same number of voxels which have the highest responses to faces from the other session; and then calculated the proportion of overlap between the two sets of voxels. The consistency score was the average proportion overlap between both session orders (session 1 first or session 2 first). We used this procedure instead of using the same threshold levels to prevent the effect of threshold on the number of voxels selected across sessions.

3. Results

The FPS-face condition successfully localized a peak of activation in the right mid-Fusiform gyrus (right "FFA") in all the young ($n = 9$) and elderly ($n = 4$) control participants. The young controls have an average coordinate of the peak FFA voxel of (41.4 ± 6.0, −52.6 ± 4.7, −11.3 ± 4.3, in Talairach coordinates), and the elderly controls have an average coordinate of the peak FFA voxel of (40.7 ± 5.2, −52.5 ± 5.6, −13.0 ± 1.4). Such peak FFA coordinates are consistent with our recent study with the FPS-fMRI face localizer (42, −54, −14, in Talairach coordinates, averaged across 12 young adults, Gao et al., 2018), as well as other previous studies (e.g., Kanwisher et al., 1997: 40, −55, −10; see also Jonas et al., 2016 in intracerebral recordings: 41, −45, −16).

3.1. *The cortical face-selective network of patient PS*

Fig. 3 shows the face-selective clusters localized by the FPS-face stimulation sequence using a threshold of $p < .0001$ (uncorrected) and a minimal cluster size of 10 voxels. Table 1 provides a summary of each cluster's size, response magnitude and Talairach Coordinates (of the peak voxel). The clusters are located in the right middle fusiform gyrus, the bilateral posterior superior temporal sulcus, the bilateral inferior frontal gyrus, the bilateral transverse superior occipital sulcus, and the right anterior occipito-temporal sulcus, as commonly seen in typical adults (Gao et al., 2018). At a more liberal threshold ($p < .01$), we identified three additional clusters in the left anterior occipito-temporal sulcus and bilateral temporal pole. There are no face-selective responses in the right inferior occipital gyrus and left-middle fusiform gyrus because of PS's brain damage. The Talairach coordinates of the peak voxel in the right fusiform gyrus of PS, i.e., the right FFA (44, −53, −17), are consistent with the average FFA coordinates of both the young and elderly controls (i.e., well within 2SDs of the controls in each of the 3 directions).

3.2. *Are PS's face-selective responses driven by low-level visual cues?*

In sharp contrast to the set of regions revealed by the FPS-face condition, the FPS-scrambled condition did not reveal *any* "functionally-active" cluster even at a more liberal threshold ($p < .001$ uncorrected and a minimal cluster size of 10 voxels). Fig. 4 shows the SNR spectrum of the BOLD response time

Please cite this article as: Gao, X et al., The cortical face network of the prosopagnosic patient PS with fast periodic stimulation in fMRI, Cortex, https://doi.org/10.1016/j.cortex.2018.11.008

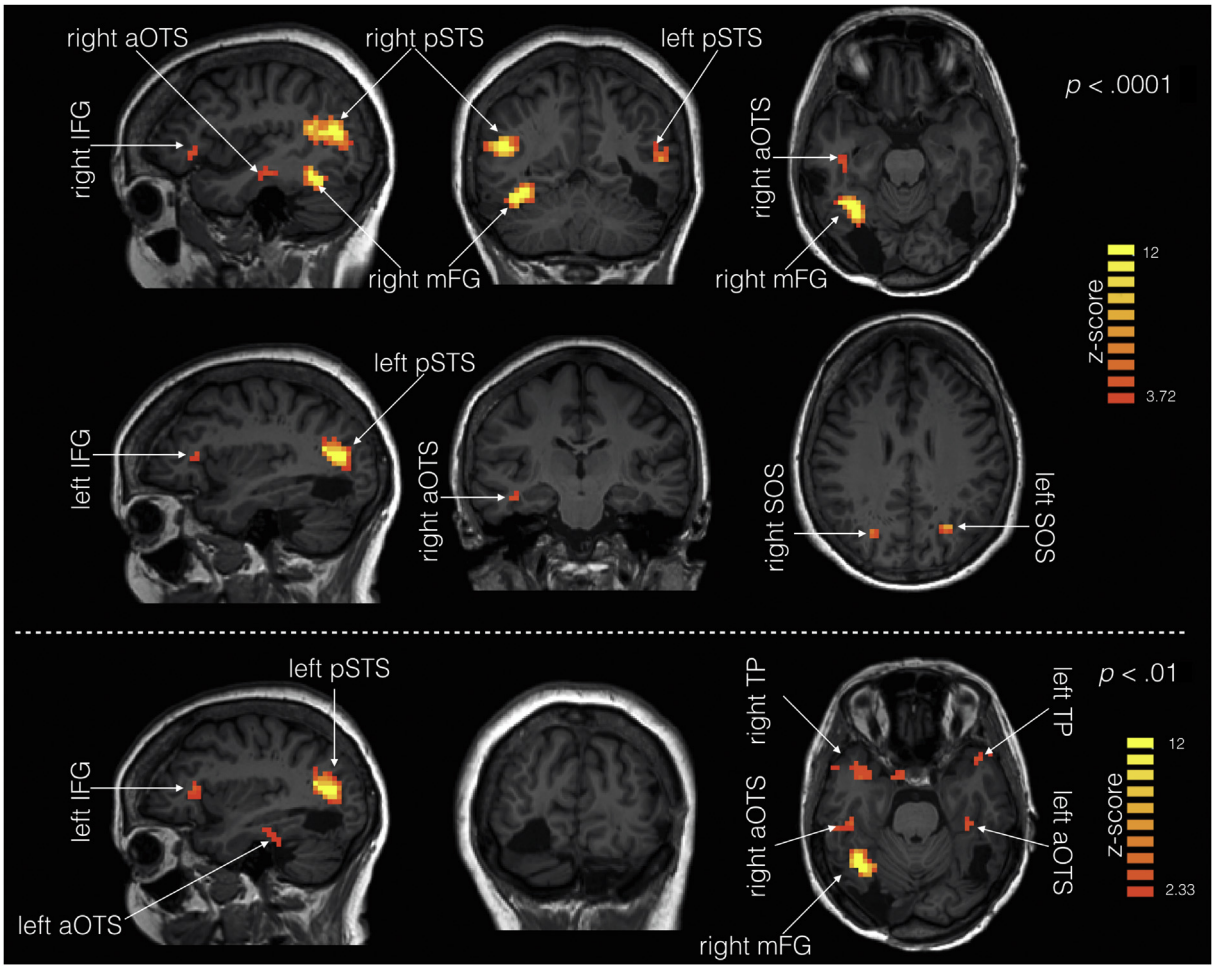

Fig. 3 – The face-selective network in PS's brain as identified by the FPS face localizer. In the top panel, the maps are thresholded at p < .0001, uncorrected, with a minimal cluster size of 10 voxels. In the bottom panel, the maps are thresholded at p < .01, uncorrected. mFG: middle Fusiform Gyrus; pSTS: posterior Superior Temporal Sulcus; IFG: Inferior Frontal Gyrus; aOTS: anterior Occipito-Temporal Sulcus; TP: Temporal Pole; SOS, transverse Superior Occipital Sulcus; TP: Temporal Pole.

Table 1 – Face-selective clusters (at $p < .0001$ and minimal cluster size of 10 3 × 3 × 3 mm^3 voxels) in PS identified with the FPS-face paradigm.

Clusters	Talairach Coordinates			Size (voxels)	Strength (max z-score)
	x	y	z		
Right pSTS	49	−73	8	305	23.0
Left pSTS	−37	−77	7	186	17.1
Right mFG	44	−53	−17	104	19.3
Left SOS	−26	−73	20	21	8.5
Right IFG	42	24	−2	19	5.3
Left IFG	−44	27	1	17	4.9
Right SOS	26	−73	22	13	6.3
Right aOTS	26	21	−9	11	6.1

Note: The Talairach coordinates are for the peak voxel in each cluster. pSTS: posterior Superior Temporal Sulcus; mFG: middle Fusiform Gyrus; SOS, transverse Superior Occipital Sulcus; IFG: Inferior Frontal Gyrus; aOTS: anterior Occipito-Temporal Sulcus.

course of the peak face-selective voxel in each face-selective cluster as identified in Fig. 3 for the different conditions. Consistent with the cluster analysis, the SNR is high at the face stimulation frequency (.111 Hz) for the FPS-face condition, and there is no increased amplitude at the same frequency for the FPS-scrambled condition. The results from the FPS-scrambled condition (in comparison to the FPS-face condition) rule out the contribution of low-level visual cues to face-selective responses observed in patient PS's brain.

3.3. *Spatial extent and reliability of PS's face selective responses in the fusiform gyrus*

With a highly conservative threshold, the face-selective response can be reduced to a single voxel, which is localized 6 mm from the anterior border of the lesion (Fig. 5). This peak localization is highly similar to previous reports (see Fig. 1 shown here, from Rossion et al., 2003; Talairach coordinates: 44, −53, −17 in the current study *vs* 42, −59, −18 in Rossion et al., 2003). However, with the conventional threshold used, given the high sensitivity of the present paradigm, the face-selective responses in the middle lateral fusiform gyrus extend to the anterior border of brain damage, i.e., extending

Please cite this article as: Gao, X et al., The cortical face network of the prosopagnosic patient PS with fast periodic stimulation in fMRI, Cortex, https://doi.org/10.1016/j.cortex.2018.11.008

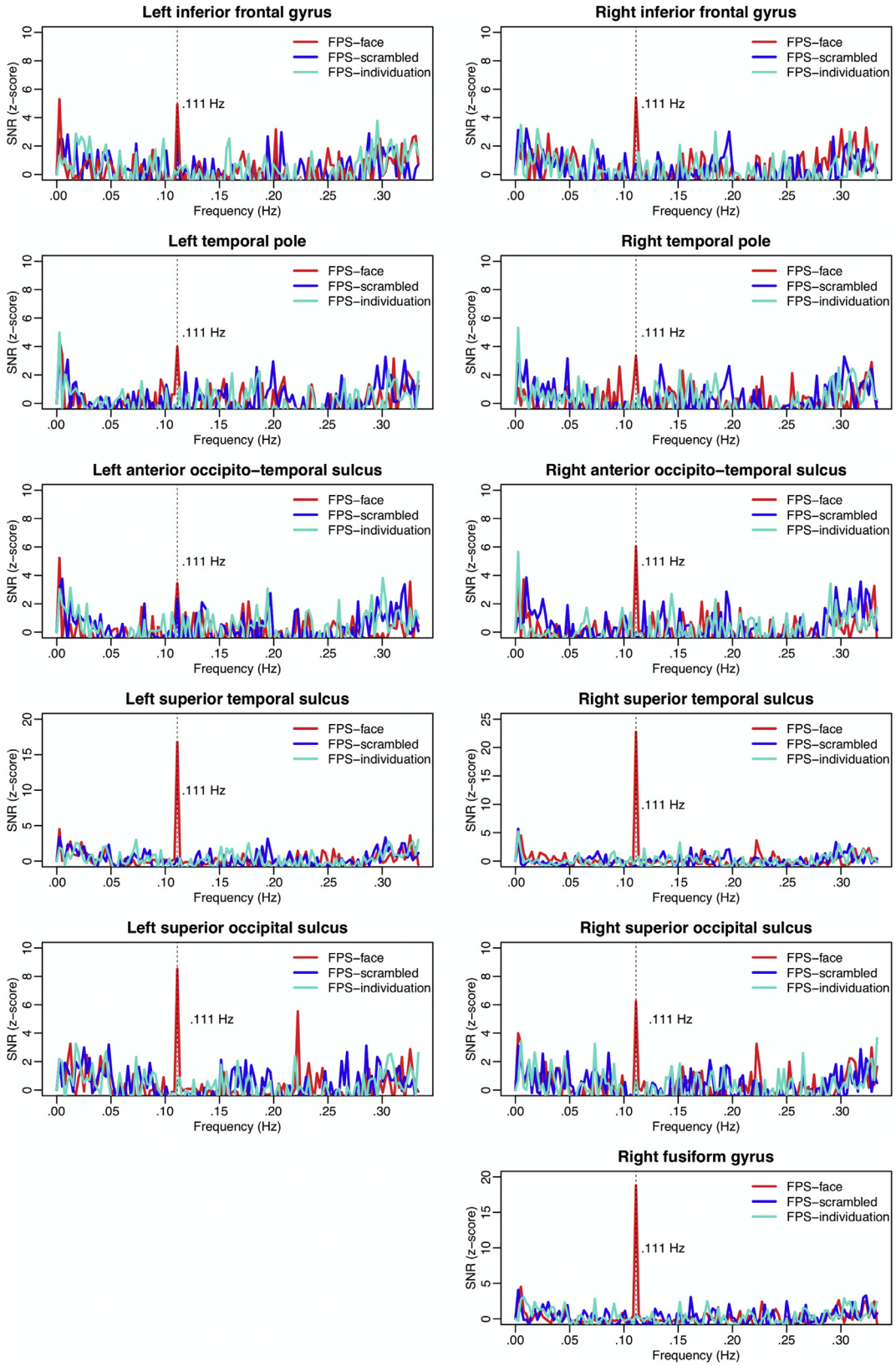

Fig. 4 – Signal-to-noise ratio (SNR) at the whole fMRI spectrum of frequencies in face-selective clusters in PS's brain, showing the peak of activation at .111 Hz. Note the second harmonic (2F = .222 Hz) bilaterally in the superior occipital sulcus region, suggesting that the shape of the BOLD response in this region differs from that of the other face-selective regions. SNR was calculated based on the BOLD response time course of the peak face-selective voxel in each cluster. The three colors represent the three different experimental conditions: FPS-face (red), FPS-scrambled (blue), and FPS-individuation (turquoise). The vertical dotted lines mark the target frequency (.111 hz).

Please cite this article as: Gao, X et al., The cortical face network of the prosopagnosic patient PS with fast periodic stimulation in fMRI, Cortex, https://doi.org/10.1016/j.cortex.2018.11.008

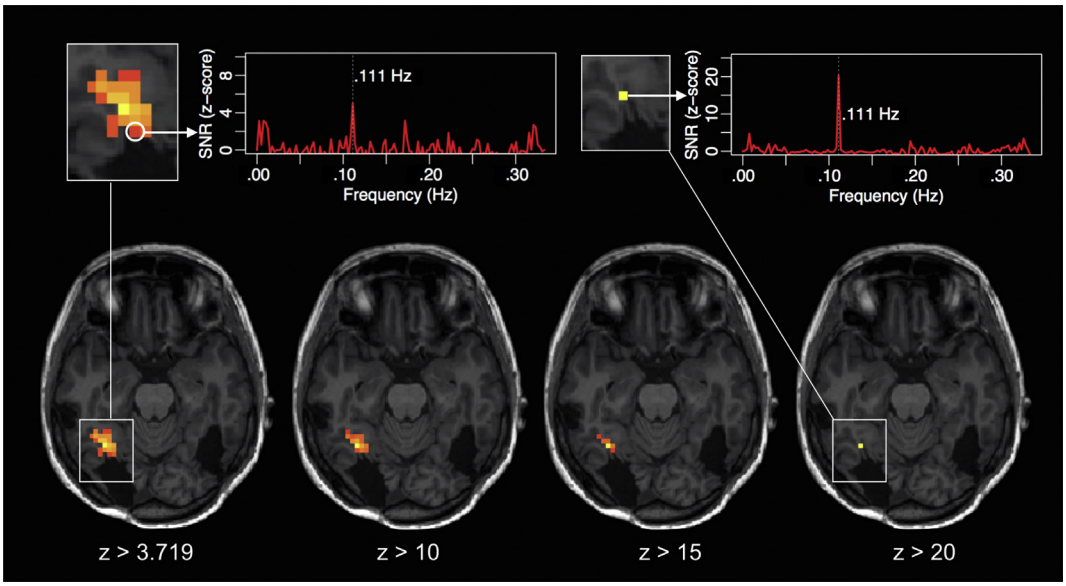

Fig. 5 – The effect of threshold in identifying face-selective voxels in PS's brain. The SNR spectrum on the top-left shows response at the face stimulation frequency of a voxel close to the lesion. The SNR spectrum on the top-right shows response at the face stimulation frequency of the peak voxel in the right fusiform gyrus.

slightly more posteriorly than in previous reports (Rossion et al., 2003; Schiltz et al., 2006; Sorger et al., 2007; Dricot et al., 2008; see Fig. 1). Importantly, the voxel lying next to the lesion is clearly above noise level (Fig. 5), suggesting that this posterior extension is genuine and observed here due to the increase in sensitivity of the FPS-Face paradigm.

For PS, we identified 87 face selective voxels in Session 1 in the right fusiform gyrus. Out of 87 voxels with the highest response amplitude in Session 2, 70 overlapped with Session 1, resulting in a consistency score of .80. Conversely, there were 46 face-selective voxels identified in Session 2. Out of 46 voxels with the highest response amplitude in Session 1, 42 overlapped with those in Session 2, resulting in a consistency score of .91. Thus, overall, PS had a consistency score of .86, suggesting a high test-retest spatial reliability.

We also assessed the spatial reliability of the controls in a similar way between two scanning runs. The consistency scores ranged from .63 to .85 (mean = .76 ± .07) for the young controls and from .67 to .79 (mean = .74 ± .05) for the elderly controls. For a fair comparison with PS, we recalculated the reliability score of PS between the two scanning runs in Session 1. We achieved a reliability score of .78 for PS, which is not significantly different from the consistency score of either the young controls or the elderly controls (*ps* = n.s., Crawford-Garthwaite Bayesian test for single-case *vs* control group, Crawford & Garthwaite, 2007). Overall, as in our previous study using the same FPS-fMRI paradigm (Gao et al., 2018), we achieved a very high test-retest reliability in defining spatial map of face-selective neural response in the right fusiform gyrus.

3.4. *Lack of face-selective responses in the occipital region*

Although the left inferior occipital gyrus is largely unaffected by brain damage, there was no face-selective response in this region of PS's brain, even with increased sensitivity in this paradigm, at a liberal threshold ($p < .01$, uncorrected; see Fig. 3 bottom panel). Thus, as in previous reports using standard fMRI paradigms, there is no right OFA, left FFA, or left OFA in the patient's brain.

3.5. *Face-selective responses in the ventral anterior temporal lobe*

Clear face-selective responses are found in the ventral anterior temporal lobe of PS's brain for the first time, specifically in the anterior *occipito-temporal sulcus*, bilaterally with a right hemispheric advantage (the left anterior *occipito-temporal sulcus* cluster only appears at a lower threshold, see Fig. 3 bottom panel). A few face-selective clusters are also found in the temporal pole, at a lower threshold ($p < .01$, uncorrected).

3.6. *Lack of response to changes in face identity in PS*

There were no identity-selective clusters in PS's brain for the FPS-individuation condition, even at a liberal threshold ($p < .01$, uncorrected, with a minimal cluster size of 10 voxels). Furthermore, there was no significant signal for face discrimination in any of the face-selective areas identified in the PS's brain from the FPS-face condition (Fig. 6).

As shown in Fig. 6, in the FPS-face condition, high SNR is seen at the target stimulation frequency (.111 Hz) in all the participants, including PS. Here we only used data from two FPS-face runs in the first scanning session for PS to allow a fair comparison with the control participants, who only underwent two FPS-face runs. While the elderly control group did show reduced peak FFA activity in comparison to the young adults ($p = .033$, Wilcoxon rank sum test), PS's peak FFA activity was not different from the young adults ($p = .386$, Crawford-Garthwaite Bayesian test for single-case *vs* control

Please cite this article as: Gao, X et al., The cortical face network of the prosopagnosic patient PS with fast periodic stimulation in fMRI, Cortex, https://doi.org/10.1016/j.cortex.2018.11.008

group, Crawford & Garthwaite, 2007). In fact, PS's peak FFA activity is marginally higher than the elderly controls ($p = .053$, Crawford-Garthwaite Bayesian test). In contrast, in the FPS-individuation condition, we found high SNR at the target stimulation frequency for all the control participants (above a z-score threshold of 3.719, $p < .0001$), but not for PS. The young adult control group did not differ from the elderly control group in the peak SNR for the FPS-individuation condition in the right fusiform gyrus ($p = .148$, Wilcoxon rank sum test). The SNR of PS is therefore significantly lower than the mean SNR of the group as a whole ($p = .041$, Crawford-Garthwaite Bayesian test), or even either the young adult controls ($p = .031$, Crawford-Garthwaite Bayesian test) alone, or the elderly controls alone ($p = .026$, Crawford-Garthwaite Bayesian test). Furthermore, a Crawford–Howell *t*-test for dissociation (Crawford-Howell, 1998) comparing PS and the elderly controls suggested that PS's score is significantly altered on the FPS-individuation condition in comparison to the FPS-face condition [$t(3) = 4.27$, $p < .05$] In sum, PS does not differ in magnitude of face-selective response in the right

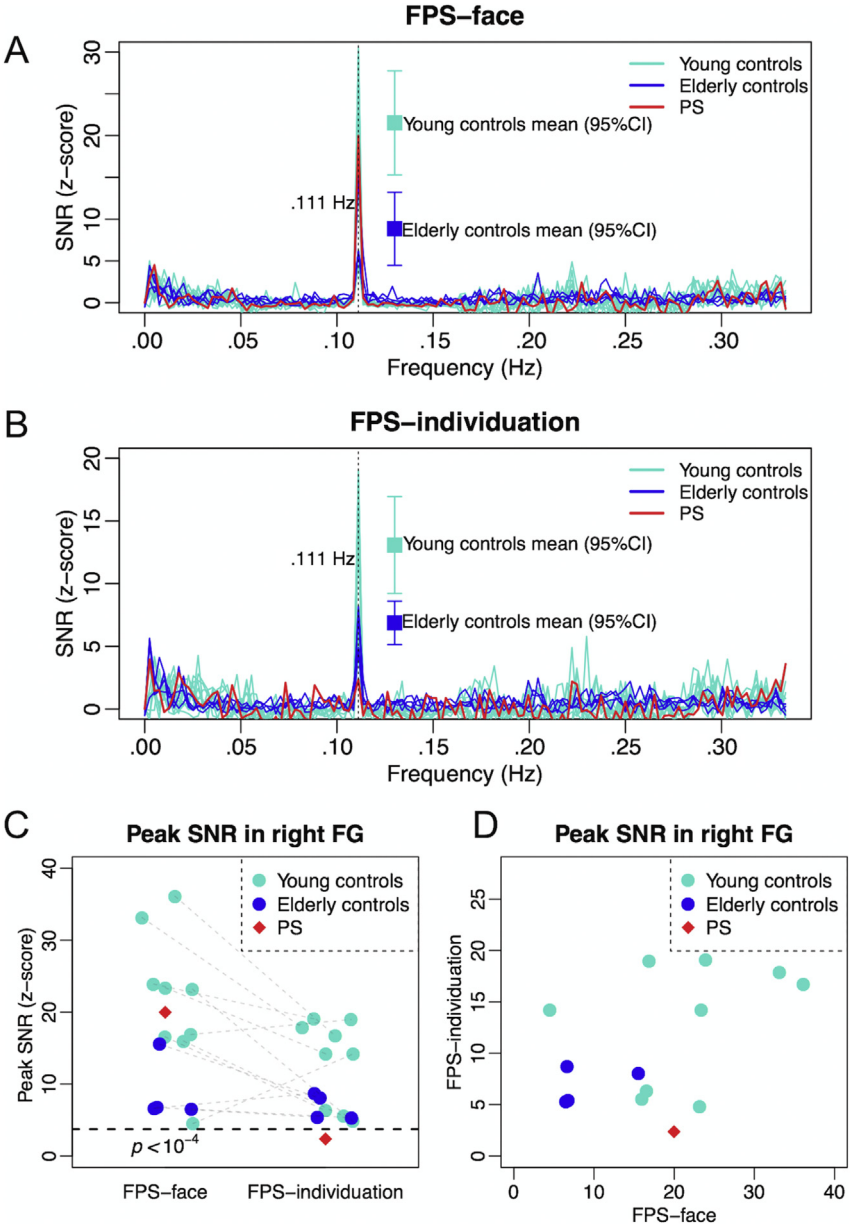

Fig. 6 – Signal-to-noise ratio (SNR) spectrum of the FPS-face condition (A) and the FPS-individuation condition (B). The red lines represent PS. The blue lines represent four elderly control participants. The turquoise lines represent nine younger control participants. The data were from the BOLD response time course of the voxels having the highest SNR in the FPS-face condition or the FPS-individuation condition, within anatomically defined right fusiform gyrus. The maximum SNR of each individual participant in the two tasks were plotted in the bottom panels. In panel C, the two data points for the two conditions for each control participants (blue or turquoise) were linked by a dashed line. The horizontal dotted line represents a threshold level of $p < .0001$. In panel D, Peak SNR of the two conditions defined the two axes.

Please cite this article as: Gao, X et al., The cortical face network of the prosopagnosic patient PS with fast periodic stimulation in fMRI, Cortex, https://doi.org/10.1016/j.cortex.2018.11.008

fusiform gyrus compared to normal controls, but is the only participant not showing a response to changes in facial identity.

4. Discussion

The paradigm to measure generic face categorization relying on fast periodic stimulation is associated with high sensitivity, specificity and reliability in fMRI signal (Gao et al., 2018), making it an ideal tool to define the cortical face network in single neurological patients for instance. Here, testing the prosopagnosic patient PS with this paradigm for the first time both supports previous observations and reveals new findings.

First, the study confirms that typical face-selective responses can be observed in the patient's brain for natural images of faces presented extremely rapidly, i.e., allowing only one fixation per face. Outside of brain damage, the localization of the face-selective regions is not different in the patient than in typical individuals, with significant clusters in the right fusiform gyrus ("FFA"), but also the bilateral posterior superior temporal sulcus, the bilateral inferior frontal gyrus, the bilateral transverse superior occipital sulcus, and the right anterior occipito-temporal sulcus. This suggests that the specific spatial topography for face-selective responses obtained in this patient with a similar approach in EEG (Liu-Shuang et al., 2016) may be due to a distortion of the outward flux of currents due to brain damage rather than differences in the localization of the remaining underlying cortical sources.

Second, our observations show that face-selective responses in PS's brain cannot be accounted for by low-level visual cues, or statistical image properties differing between faces and objects contained in the amplitude spectrum (see Crouzet & Thorpe, 2011; Van Rullen, 2006). This observation does not support the view that statistical image properties play a significant role in category-selective responses in the ventral visual stream, in particular for faces (Andrews et al., 2015; Rice, Watson, Hartley, & Andrews, 2014). Note that this latter view is based on observations made with stimulus sets composed of segmented objects that are much more homogenous *within* a category in terms of low-level properties, emphasizing inter-category differences in such properties. In contrast, in the large natural stimulus set used here, exemplars of both faces and objects vary widely in terms of low-level visual cues, minimizing systematic differences between the two sets. Moreover, previous studies were conducted with standard localizer tasks (i.e., block designs), which are more sensitive to such confounds: even with our widely variable image set, increases of activity in low-level visual regions can be found in fMRI when they are tested in a conventional block design stimulation mode (see Gao et al., 2018).

Third, we find PS's peak of face-selectivity in the right fusiform gyrus at the same localization as the controls as well as in previous studies performed with this patient (e.g., Talairach coordinates of 42, −59, −18 in Rossion et al., 2003, p. 36, −54, −20 in Sorger et al., 2007, p. 44, −53, −17 in the present study). However, interestingly, we show here thanks to a highly sensitive paradigm that this region as a whole form a continuous patch of activation starting at the very anterior edge of the right inferior occipital gyrus/posterior fusiform lesion and extending anteriorly along the lateral fusiform gyrus. In other words, there is no "gap" in activation, as previously thought, between the lesion and the face-selective activation in the right fusiform gyrus (right "FFA"; Fig. 5). Importantly, this extension of the fusiform face-selective activation compared to previous reports cannot be attributed to a lack of specificity of the paradigm (i.e., sensitivity to low-level visual cues). The fact that face-selective activity is found at the edge of the brain lesion suggests that brain damage may have directly affected face-selective neural tissue between the right OFA and FFA. Alternatively, it could be that this extent of the face-selective response is specific to the patient PS's brain, i.e., that the recruitment of face-selective populations of neurons extended (post-damage) until the posterior border of the lesion (although with no known improvement of her prosopagnosic condition).

Fourth, we failed to find face-selective responses posterior to this cluster in ventral occipital regions, neither in the right hemisphere around or posterior to the lesion, or in the left hemisphere. Given that this paradigm shows substantial increase in sensitivity over typical face localizers (Gao et al., 2018), this confirms the view that face-selective activity in the right fusiform gyrus ("FFA") does not emerge from posterior face-selective inputs, in particular from the left hemisphere, and supports the non-hierarchical view of the cortical face network (Duchaine & Yovel, 2015; Rossion, 2008; Rossion et al., 2003).

Fifth, we report for the first time that face-selective activation in the anatomically intact ventral anterior temporal lobe of the patient PS, a region that is notoriously difficult to sample in fMRI due to large magnetic susceptibility artifacts (e.g., Jonas et al., 2015; Wandell, 2011). Moreover, face-selectivity was also found in the temporal pole, bilaterally, although the clusters were of relatively small size in these regions. These observations confirm that PS's occipito-temporal cortex anterior to the inferior occipital gyrus in the right hemisphere and to the fusiform gyrus in the left hemisphere is intact, both structurally and functionally (as far as face-selectivity is concerned). This dismisses suggestions that the patient has damage in the right anterior temporal lobe "potentially contributing to her prosopagnosia" (Pitcher et al., 2011), a claim made on the basis of a lesion in the *lateral* section of the *middle* temporal gyrus, outside of the cortical face network and visible on Fig. 3.

Despite a growing interest in recent years, the role(s) of the ventral anterior temporal regions, including the temporal pole, in face processing, remains unclear. While it has been suggested that these regions play a key role in face identity coding in the normal brain (Li et al., 2016; Nasr & Tootell, 2012; Haxby and Gobbini, 2000; Von Der Heide et al., 2013; Yang et al., 2016), here there was no sensitivity to differences between individual faces in this region of the patient PS's brain. Although this absence of sensitivity to individual face discrimination in the ventral anterior temporal lobe is in line with the patient's prosopagnosia, it contrasts with previous observations of preserved face-selectivity and sensitivity to individual faces in an fMR-adaptation paradigm in another

Please cite this article as: Gao, X et al., The cortical face network of the prosopagnosic patient PS with fast periodic stimulation in fMRI, Cortex, https://doi.org/10.1016/j.cortex.2018.11.008

case of prosopagnosia with posterior damage to the right FFA and OFA (Yang et al., 2016) as well as larger responses to familiar than unfamiliar faces in another case of prosopagnosia (Valdés-Sosa et al., 2011). Here, in fact there was no evidence of sensitivity to individual faces anywhere in the patient's brain, in line with previous fMRI studies of the patient (Schiltz et al., 2006; Dricot et al., 2008; Steeves et al., 2009 in more classical fMRI-adaptation paradigms) as well as the lack of effect in a similar paradigm as used in EEG with the same patient PS (Liu-Shuang et al., 2016). This observation is unlikely to be due to a lack of sensitivity to this paradigm, which provides significant effects in every individual tested, including the 4 age-matched controls, who were undistinguishable from the younger controls in the individual face discrimination task.

Besides differences between neurological patients, a potential reason for this difference is that unfamiliar faces were used here, while these previous studies used familiar faces (even though it is difficult to understand how patients with prosopagnosia, who do not recognize these familiar faces, may show sensitivity to individuality restricted to such familiar faces). Another potential reason for this discrepancy is that the fast periodic visual stimulation paradigm used here put stronger time constraints than typical fMRI-adaptation paradigms, since individual faces have to be discriminated at a single glance, being presented for a very brief time and at a fast rate of 6 Hz.

In summary, our study shows that the FPS-fMRI approach identifying the neural network involved in generic face categorization in the human healthy brain (Gao et al., 2018) is particularly well-suited to identify these remaining functional responses in a single neurological case, here the patient PS, studied extensively in behavioral and neural studies. Our findings do not only support previous observations but reveal for the first time the larger extent of the face-selective activation in the lateral section of the right middle fusiform gyrus (i.e., right FFA) which appear to forms a reliable single cluster of activation lying at the anterior border of the patient's main lesion in the inferior occipital gyrus, and rule out the contributions of low-level visual cues and posterior face-selective activation in the patient's brain. The sensitive face localizer approach also reveals an intact face-selective network anterior to the fusiform gyrus, including clusters in the ventral anterior temporal lobe (occipito-temporal sulcus and temporal pole) and the inferior frontal gyrus, with a right hemispheric dominance. The novel FPS-FMRI paradigm testing sensitivity to changes of unfamiliar face identities across size changes appears extremely promising, revealing significant responses in all individuals tested in the right FFA, but for the patient, in line with her prosopagnosia.

Acknowledgements

This work was supported by a grant from the Fonds National de la Recherche Scientifique (FNRS, Belgium), an Economic and Social Research Council grant [ES/J009075/1] to QCV and BR, and a postdoctoral UCL/Marie-Curie fellowship to XG. We thank two anonymous reviewers for their constructive comments on a previous version of the paper.

Appendix

Benton Facial Recognition Test: in this test, participants perform a face matching task. In each trial, one target face is presented above six test faces, which contains one to three target faces. The target faces can vary in pose and lighting. Male and female faces are used. Clothing and hair cures are removed from the faces. There is a short form with 27 possible points and a long form with 54 possible points. Both accuracy and response time are recorded.

Cambridge Face Memory Test: in this test, participants are introduced to six target faces, and then they are tested with a three alternative forced choice paradigm to identify one target face among two distractor faces. Each target face is presented three times with the identical views to those studied in the introduction, five times with novel views, and four times with novel views plus noise. In total, there are 72 trials. Only male faces are used in this test. Both accuracy and response time are recorded.

Declarations of interest

None.

REFERENCES

Andrews, T. J., Watson, D. M., Rice, G. E., & Hartley, T. (2015). Low-level properties of natural images predict topographic patterns of neural response in the ventral visual pathway. *Journal of Vision, 15*(7), 3. https://doi.org/10.1167/15.7.3.

Axelrod, V., & Yovel, G. (2013). The challenge of localizing the anterior temporal face area: A possible solution. *Neuroimage, 81*, 371–380. https://doi.org/10.1016/j.neuroimage.2013.05.015.

Barton, J. J. S. (2008). Prosopagnosia associated with a left occipitotemporal lesion. *Neuropsychologia, 46*(8), 2214–2224. https://doi.org/10.1016/j.neuropsychologia.2008.02.014.

Benton, A. L., & Van Allen, M. W. (1972). Prosopagnosia and facial discrimination. *Journal of the Neurological Sciences, 15*(2), 167–172. https://doi.org/10.1016/0022-510X(72)90004-4.

Berman, M. G., Park, J., Gonzalez, R., Polk, T. A., Gehrke, A., Knaffla, S., et al. (2010). Evaluating functional localizers: The case of the FFA. *Neuroimage, 50*(1), 56–71. https://doi.org/10.1016/j.neuroimage.2009.12.024.

Bodamer, J. (1947). Die prosop-agnosie. *Archiv Für Psychiatrie Und Nervenkrankheiten Vereinigt Mit Zeitschrift Für Die Gesamte Neurologie Und Psychiatrie, 179*(1–2), 6–53. https://doi.org/10.1007/BF00352849.

Bouvier, S. E., & Engel, S. A. (2006). Behavioral deficits and cortical damage loci in cerebral achromatopsia. *Cerebral Cortex, 16*(2), 183–191. https://doi.org/10.1093/cercor/bhi096.

Busigny, T., Graf, M., Mayer, E., & Rossion, B. (2010). Acquired prosopagnosia as a face-specific disorder: Ruling out the general visual similarity account. *Neuropsychologia, 48*(7), 2051–2067. https://doi.org/10.1016/j.neuropsychologia.2010.03.026.

Busigny, T., Prairial, C., Nootens, J., Kindt, V., Engels, S., Verplancke, S., et al. (2014). CELEB: A neuropsychological tool for famous face recognition and proper name production. *Revue de Neuropsychologie, 6*, 69–81.

Caldara, R., Schyns, P., Mayer, E., Smith, M. L., Gosselin, F., & Rossion, B. (2005). Does prosopagnosia take the eyes out of

face representations? Evidence for a defect in representing diagnostic facial information following brain damage. *Journal of Cognitive Neuroscience, 17*, 1652–1666. https://doi.org/10.1162/089892905774597254.

Collins, J. A., Koski, J. E., & Olson, I. R. (2016). More than meets the eye: The merging of perceptual and conceptual knowledge in the anterior temporal face area. *Frontiers in Human Neuroscience, 10*. https://doi.org/10.3389/fnhum.2016.00189.

Collins, J. A., & Olson, I. R. (2014). Beyond the FFA: The role of the ventral anterior temporal lobes in face processing. *Neuropsychologia, 61*, 65–79. https://doi.org/10.1016/j.neuropsychologia.2014.06.005.

Crawford, J. R., & Garthwaite, P. H. (2007). Comparison of a single case to a control or normative sample in neuropsychology: Development of a Bayesian approach. *Cognitive Neuropsychology, 24*, 343–372.

Crawford, J. R., & Howell, D. C. (1998). Comparing an individual's test score against norms derived from small samples. *The Clinical Neuropsychologist, 12*, 482–486.

Crouzet, S. M., & Thorpe, S. J. (2011). Low-level cues and ultra-fast face detection. *Frontiers in Psychology, 2*, 342. https://doi.org/10.3389/fpsyg .2011.00342.

Dricot, L., Sorger, B., Schiltz, C., Goebel, R., & Rossion, B. (2008). The roles of "face" and "non-face" areas during individual face perception: Evidence by fMRI adaptation in a brain-damaged prosopagnosic patient. *Neuroimage, 40*(1), 318–332. https://doi.org/10.1016/j.neuroimage.2007.11.012.

Duchaine, B., & Nakayama, K. (2006). The Cambridge face memory test: results for neurologically intact individuals and an investigation of its validity using inverted face stimuli and prosopagnosic participants. *Neuropsychologia, 44*(4), 576–585.

Duchaine, B., & Yovel, G. (2015). A revised neural framework for face processing. *Annual Review of Vision Science, 1*(1), 393–416. https://doi.org/10.1146/annurev-vision-082114-035518.

Duncan, K. J., Pattamadilok, C., Knierim, I., & Devlin, J. T. (2009). Consistency and variability in functional localisers. *Neuroimage, 46*(4), 1018–1026. https://doi.org/10.1016/j.neuroimage.2009.03.014.

Dzhelyova, M., & Rossion, B. (2014). Supra-additive contribution of shape and surface information to individual face discrimination as revealed by fast periodic visual stimulation. *Journal of Vision, 14*(14), 15, 1–14.

Fairhall, S. L., & Ishai, A. (2007). Effective connectivity within the distributed cortical network for face perception. *Cerebral Cortex, 17*(10), 2400–2406. https://doi.org/10.1093/cercor/bhl148.

Gao, X., Gentile, F., & Rossion, B. (2018). Fast periodic stimulation (FPS): A highly effective approach in fMRI brain mapping. *Brain Structural and Function, 223*, 2433–2454. https://doi.org/10.1007/s00429-018-1630-4.

Gentile, F., & Rossion, B. (2017). Being BOLD: The neural dynamics of face perception. *Human Brain Mapping, 38*, 120–139. https://doi.org/10.1002/hbm.23348.

Germine, L. T., Duchaine, B., & Nakayama, K. (2011). Where cognitive development and aging meet: Face learning ability peaks after age 30. *Cognition, 118*, 201–210.

Haxby, H., & Gobbini. (2000). The distributed human neural system for face perception. *Trends in Cognitive Sciences, 4*(6), 223–233.

Hecaen, H., & Angelergues, R. (1962). Agnosia for faces (prosopagnosia). *Archives of Neurology, 7*(2), 92–100. https://doi.org/10.1001/archneur.1962.04210020014002.

Ishai, A. (2008). Let's face it: it's a cortical network. *Neuroimage, 40*(2), 415–419. https://doi.org/10.1016/j.neuroimage.2007.10.040.

Jiang, F., Dricot, L., Weber, J., Righi, G., Tarr, M. J., Goebel, R., et al. (2011). Face categorization in visual scenes may start in a higher order area of the right fusiform gyrus: Evidence from dynamic visual stimulation in neuroimaging. *Journal of Neurophysiology, 106*(5), 2720–2736. https://doi.org/10.1152/jn.00672.2010.

Jonas, J., Brissart, H., Hossu, G., Colnat-Coulbois, S., Vignal, J. P., Rossion, B., et al. (2018). A face identity hallucination (palinopsia) generated by intracerebral stimulation of the face-selective right lateral fusiform cortex. *Cortex, 99*, 296–310. https://doi.org/10.1016/j.cortex.2017.11.022.

Jonas, J., Jacques, C., Liu-Shuang, J., Brissart, H., Colnat-Coulbois, S., Maillard, L., et al. (2016). A face-selective ventral occipito-temporal map of the human brain with intracerebral potentials. *Proceedings of the National Academy of Sciences, 113*(28), E4088–E4097. https://doi.org/10.1073/pnas.1522033113.

Jonas, J., Rossion, B., Brissart, H., Frismand, S., Jacques, C., Hossu, G., et al. (2015). Beyond the core face-processing network: Intracerebral stimulation of a face-selective area in the right anterior fusiform gyrus elicits transient prosopagnosia. *Cortex, 72*, 140–155. https://doi.org/10.1016/j.cortex.2015.05.026.

Kanwisher, N. (2017). The quest for the FFA and where it led. *The Journal of Neuroscience, 37*(5), 1056–1061. https://doi.org/10.1523/JNEUROSCI.1706-16.2016.

Kanwisher, N., McDermott, J., & Chun, M. M. (1997). The fusiform face area: A module in human extrastriate cortex specialized for face perception. *The Journal of Neuroscience , 17*(11), 4302–4311. https://doi.org/10.1098/Rstb.2006.1934.

Kawabata Duncan, K. J., & Devlin, J. T. (2011). Improving the reliability of functional localizers. *Neuroimage, 57*(3), 1022–1030. https://doi.org/10.1016/j.neuroimage.2011.05.009.

Li, J., Dong, M., Ren, A., Ren, J., Zhang, J., & Huang, L. (2016). Structural attributes of the temporal lobe predict face recognition ability in youth. *Neuropsychologia, 84*, 1–6. https://doi.org/10.1016/j.neuropsychologia.2016.01.024.

Liu-Shuang, J., Norcia, A. M., & Rossion, B. (2014). An objective index of individual face discrimination in the right occipito-temporal cortex by means of fast periodic oddball stimulation. *Neuropsychologia, 52*(1), 57–72. https://doi.org/10.1016/j.neuropsychologia.2013.10.022.

Liu-Shuang, J., Torfs, K., & Rossion, B. (2016). An objective electrophysiological marker of face individualisation impairment in acquired prosopagnosia with fast periodic visual stimulation. *Neuropsychologia, 83*, 100–113. https://doi.org/10.1016/j.neuropsychologia.2015.08.023.

McCarthy, G., Spicer, M., Adrignolo, A., Luby, M., Gore, J., & Allison, T. (1994). Brain activation associated with visual motion studied by functional magnetic resonance imaging in humans. *Human Brain Mapping, 2*(4), 234–243. https://doi.org/10.1002/hbm.460020405.

Meadows, J. C. (1974). The anatomical basis of prosopagnosia. *Journal of Neurology Neurosurgery and Psychiatry, 37*(5), 489–501. https://doi.org/10.1136/jnnp.37.5.489.

Nasr, S., & Tootell, R. B. H. (2012). Role of fusiform and anterior temporal cortical areas in facial recognition. *Neuroimage, 63*(3), 1743–1753. https://doi.org/10.1016/j.neuroimage.2012.08.031.

Parvizi, J., Jacques, C., Foster, B. L., Withoft, N., Rangarajan, V., Weiner, K. S., et al. (2012). Electrical stimulation of human fusiform face-selective regions distorts face perception. *Journal of Neuroscience, 32*(43), 14915–14920. https://doi.org/10.1523/JNEUROSCI.2609-12.2012.

Pitcher, D., Dilks, D. D., Saxe, R. R., Triantafyllou, C., & Kanwisher, N. (2011). Differential selectivity for dynamic versus static information in face-selective cortical regions. *Neuroimage, 56*(4), 2356–2363. https://doi.org/10.1016/j.neuroimage.2011.03.067.

Pitcher, D., Walsh, V., & Duchaine, B. (2011). The role of the occipital face area in the cortical face perception network. *Experimental Brain Research, 209*(4), 481–493. https://doi.org/10.1007/s00221-011-2579-1.

Please cite this article as: Gao, X et al., The cortical face network of the prosopagnosic patient PS with fast periodic stimulation in fMRI, Cortex, https://doi.org/10.1016/j.cortex.2018.11.008

Prieto, E. (2011). Early (N170/M170) face-sensitivity despite right lateral occipital brain damage in acquired prosopagnosia. *Frontiers in Human Neuroscience,* 5. https://doi.org/10.3389/fnhum.2011.00138.

Puce, A., Allison, T., Gore, J. C., & McCarthy, G. (1995). Face-sensitive regions in human extrastriate cortex studied by functional MRI. *Journal of Neurophysiology, 74*(3), 1192–1199. Retrieved from www.ncbi.nlm.nih.gov/pubmed/7500143.

Rajimehr, R., Young, J. C., & Tootell, R. B. H. (2009). An anterior temporal face patch in human cortex, predicted by macaque maps. *Proceedings of the National Academy of Sciences, 106*(6), 1995–2000. https://doi.org/10.1073/pnas.0807304106.

Ramon, M., Busigny, T., Gosselin, F., & Rossion, B. (2016). All new kids on the block? Impaired holistic processing of personally familiar faces in a kindergarten teacher with acquired prosopagnosia. *Visual Cognition, 24*(5–6), 321–355. https://doi.org/10.1080/13506285.2016.1273985.

Rangarajan, V., Hermes, D., Foster, B. L., Weiner, K. S., Jacques, C., Grill-Spector, K., et al. (2014). Electrical stimulation of the left and right human fusiform gyrus causes different effects in conscious face perception. *Journal of Neuroscience, 34*(38), 12828–12836. https://doi.org/10.1523/JNEUROSCI.0527-14.2014.

Rice, G. E., Watson, D. M., Hartley, T., & Andrews, T. J. (2014). Low-level image properties of visual objects predict patterns of neural response across category-selective regions of the ventral visual pathway. *Journal of Neuroscience, 34*(26), 8837–8844. https://doi.org/10.1523/JNEUROSCI.5265-13.2014.

Righart, R., Andersson, F., Schwartz, S., Mayer, E., & Vuilleumier, P. (2010). Top-down activation of fusiform cortex without seeing faces in prosopagnosia. *Cerebral Cortex, 20*(8), 1878–1890. https://doi.org/10.1093/cercor/bhp254.

Rossion, B. (2008). Constraining the cortical face network by neuroimaging studies of acquired prosopagnosia. *Neuroimage,* 40(2), 423–426. https://doi.org/10.1016/j.neuroimage.2007.10.047.

Rossion, B. (2014). Understanding face perception by means of prosopagnosia and neuroimaging. *Frontiers in Bioscience Elite,* 6E(2), 258–307.

Rossion, B. (2018). Damasio's error-Prosopagnosia with intact within-category object recognition. *Journal of Neuropsychology,* 12, 357–388.

Rossion, B., Caldara, R., Seghier, M., Schuller, A.-M., Lazeyras, F., & Mayer, E. (2003). A network of occipito-temporal face-sensitive areas besides the right middle fusiform gyrus is necessary for normal face processing. *Brain, 126*(Pt 11), 2381–2395. https://doi.org/10.1093/brain/awg241.

Rossion, B., Dricot, L., Goebel, R., & Busigny, T. (2011). Holistic face categorization in higher order visual areas of the normal and prosopagnosic brain: Toward a non-hierarchical view of face perception. *Frontiers in Human Neuroscience,* 4, 225. https://doi.org/10.3389/fnhum.2010.00225.

Rossion, B., Jacques, C., & Jonas, J. (2018). Mapping face categorization in the human ventral occipitotemporal cortex with direct neural intracranial recordings. *Annals of the New York Academy of Sciences*. https://doi.org/10.1111/nyas.13596.

Rossion, B., Torfs, K., Jacques, C., & Liu-Shuang, J. (2015). Fast periodic presentation of natural images reveals a robust face-selective electrophysiological response in the human brain. *Journal of Vision,* 15(1). https://doi.org/10.1167/15.1.18, 18–18.

Schiltz, C., Sorger, B., Caldara, R., Ahmed, F., Mayer, E., Goebel, R., et al. (2006). Impaired face discrimination in acquired prosopagnosia is associated with abnormal response to individual faces in the right middle fusiform gyrus. *Cerebral Cortex,* 16(4), 574–586. https://doi.org/10.1093/cercor/bhj005.

Sergent, J., Shinsuke, O., & Macdonald, B. (1992). Functional neuroanatomy of face and object processing: A positron emission tomography study. *Brain,* 115, 15–36.

Sergent, J., & Signoret, J. L. (1992). Varieties of functional deficits in prosopagnosia. *Cerebral Cortex,* 2(5), 375–388. https://doi.org/10.1093/cercor/2.5.375.

Smith, S. M., Jenkinson, M., Woolrich, M. W., Beckmann, C. F., Behrens, T. E. J., Johansen-Berg, H., et al. (2004). Advances in functional and structural MR image analysis and implementation as FSL. *Neuroimage,* 23(Suppl. 1), S208–S219. https://doi.org/10.1016/j.neuroimage.2004.07.051.

Sorger, B., Goebel, R., Schiltz, C., & Rossion, B. (2007). Understanding the functional neuroanatomy of acquired prosopagnosia. *Neuroimage,* 35(2), 836–852. https://doi.org/10.1016/j.neuroimage.2006.09.051.

Steeves, J. K. E., Culham, J. C., Duchaine, B. C., Pratesi, C. C., Valyear, K. F., Schindler, I., et al. (2006). The fusiform face area is not sufficient for face recognition: Evidence from a patient with dense prosopagnosia and no occipital face area. *Neuropsychologia,* 44(4), 594–609. https://doi.org/10.1016/j.neuropsychologia.2005.06.013.

Steeves, J., Dricot, L., Goltz, H. C., Sorger, B., Peters, J., Milner, A. D., et al. (2009). Abnormal face identity coding in the middle fusiform gyrus of two brain-damaged prosopagnosic patients. *Neuropsychologia,* 47(12), 2584–2592. https://doi.org/10.1016/j.neuropsychologia.2009.05.005.

Valdés-Sosa, M., Bobes, M. A., Quiñones, I., Garcia, L., Valdes-Hernandez, P. A., Iturria, Y., et al. (2011). Covert face recognition without the fusiform-temporal pathways. *Neuroimage,* 57(3), 1162–1176. https://doi.org/10.1016/j.neuroimage.2011.04.057.

VanRullen, R. (2006). On second glance: Still no high-level pop-out effect for faces. *Vision Research, 46*(18), 3017–3027. https://doi.org/10.1016/j.visres.2005.07.009.

Von Der Heide, R. J., Skipper, L. M., & Olson, I. R. (2013). Anterior temporal face patches: A meta-analysis and empirical study. *Frontiers in Human Neuroscience,* 7. https://doi.org/10.3389/fnhum.2013.00017.

Wandell, B. A. (2011). The neurobiological basis of seeing words. *Annals of the New York Academy of Sciences,* 1224(1), 63–80. https://doi.org/10.1111/j.1749-6632.2010.05954.x.

Watson, D. M., Young, A. W., & Andrews, T. J. (2016). Spatial properties of objects predict patterns of neural response in the ventral visual pathway. *Neuroimage, 126*, 173–183. https://doi.org/10.1016/j.neuroimage.2015.11.043.

Weiner, K. S., Jonas, J., Gomez, J., Maillard, L., Brissart, H., Hossu, G., et al. (2016). The face-processing network is resilient to focal resection of human visual cortex. *Journal of Neuroscience,* 36(32), 8425–8440. https://doi.org/10.1523/JNEUROSCI.4509-15.2016.

Yang, H., Susilo, T., & Duchaine, B. (2016). The anterior temporal face area contains invariant representations of face identity that can persist despite the loss of right FFA and OFA. *Cerebral Cortex,* 26(3), 1096–1107. https://doi.org/10.1093/cercor/bhu289.

Young, A. W. (2011). Disorders of face perception. In A. J. Calder, G. Rhodes, J. V. Haxby, & M. H. Johnson (Eds.), *The Oxford handbook of face perception* (pp. 77–91). Oxford: Oxford University Press.

Please cite this article as: Gao, X et al., The cortical face network of the prosopagnosic patient PS with fast periodic stimulation in fMRI, Cortex, https://doi.org/10.1016/j.cortex.2018.11.008